10.5005/jp-journals-10024-2404

ORIGINAL RESEARCH

Effect of Rapid Maxillary Expansion on Condyle–fossa Relationship in Growing Patients

[1]Mona S Ghoussoub, [2]Robert Garcia, [3]Ghassan Sleilaty, [4]Khaldoun Rifai

ABSTRACT

Aim: This study tests whether rapid maxillary expansion (RME) exerts long term effects on interglenoid fossa distance and condyle fossa relationship.

Materials and methods: Consecutive growing patients aged 8 to 13 years were allocated either to the RME group or control group. Cone-beam computed tomography was performed at baseline and at 6 months. Specific software was used to determine fixed landmarks. Multivariate Analysis of Covariance (MANCOVA) models were used, with time by group interaction, using age as a covariate.

Results: Twenty-seven patients with a mean age of 11.4 ± 1.5 years were included. There was an overall significant group by time interaction (p = 0.012, effect size 0.59). Change in the lateral position of the glenoid fossa, the primary outcome, was reached (p = 0.008, effect size 0.258). Change in the laterolateral position of the center of the condyle, and the co-primary outcome was also significant (p = 0.011, effect size = 0.24). Nasal cavity width increased (p = 0.065, effect size = 0.14). There was an initial asymmetry in the horizontal position of the condyles that was carried on with no effect of RME.

Conclusion: Rapid maxillary expansion (RME) produces a significant increase in the interglenoid fossa distance and displacement of the mandibular condyles at 6 months in growing patients compared to a control group.

Clinical significance: The current study shows that RME is effective during growth, widening the interglenoid fossa distance and the lateral positions of the condyles and eventually enlarging the nasal cavity, without causing asymmetry.

Keywords: Condyle–fossa relationship, Cone-beam computer tomograph, Interglenoid fossa, Rapid maxillary expansion.

How to cite this article: Ghoussoub MS, Garcia R, Sleilaty G, Rifai K. Effect of Rapid Maxillary Expansion on Condyle–fossa Relationship in Growing Patients. The Journal of Contemporary Dental Practice, October 2018;19(10):1189-1198.

Source of support: Nil

Conflict of interest: None

[1]Department of Orthodontics, School of Dental Medicine, Hadath, Lebanon

[2]School of Dental Medicine, Paris Diderot University (Paris VII), Paris, France

[3]Department of Biostatistics, Faculty of Medicine, Saint Joseph University, Beirut, Lebanon

[4]Department of Prosthodontics, School of Dental Medicine, Hadath, Lebanon

Corresponding Author : Mona S Ghoussoub, Department of Orthodontics, School of Dental Medicine, Hadath, Lebanon, e-mail: mona_gsoub@yahoo.fr

INTRODUCTION

Maxillary palatal expansion is used to induce the rupture of the median palatine suture to correct the maxillary transverse deficiency, dental crowding, posterior crossbites, nasal resistance, or for loosening of the maxillary sutures to facilitate the correction of anteroposterior malocclusions.[1,2] Rapid maxillary expansion (RME) has been associated with improvement of impaired breathing, enuresis, and hearing loss.[3-6]

The major effect of RME is noticed in the dentition and midfacial complex,[7-9] with associated mandibular changes like increased width and spatial rotation,[10,11] changes of the condylar position relative to the glenoid fossa,[12] asymmetric corrections for unilateral crossbite,[13] symmetrical corrections for mispositioned condyles in the glenoid fossa[14] and condylar response.[15] However, the impact of RME on the glenoid fossa and the mandibular condyle is not well documented.[16-18]

This clinical trial aims to quantify the changes following RME in young subjects with significant maxillary skeletal deficiency in the transverse dimension and bilateral crossbite, comparatively to an untreated control group to adjust on variations resulting from normal growth.

MATERIALS AND METHODS

The study protocol was approved by the Research Ethics Committee of the Lebanese University, Hadath, Lebanon. (Registration number: CUEMB 31/4/2015). Informed consent was obtained from children's parents or guardians. The protocol was retrospectively registered in BMC (Bio Med Central) with ISRCTN registry: DOI 10.1186/ISRCTN77788053.[19] The screening campaign took place during 2016 and recruitment started in September 2016. Patients were recruited in the orthodontic unit and neighboring schools if they met the following inclusion criteria:

- Aged 8 to 13 years;
- Presenting a transverse maxillary skeletal deficiency, with bilateral crossbite involving one or more posterior teeth;
- Presenting a sufficient crown length (3-4 mms) to provide the necessary anchorage for the RME appliance;
- Presenting a deep palatal vault;
- Dental crowding at the start of treatment.

The subjects were excluded if they had any of the following:

- Craniofacial syndromes;
- Missing maxillary posterior permanent teeth (first molars);
- Concomitant periodontal disease;
- Previous orthodontic treatment.

The study was a two-arm, parallel group, controlled prospective clinical trial. The participants were allocated either:

- To the RME group, using an expansion device (Hyrax®, Dentaurum, Ispringen, Germany), applying the activation rate used by Primozic et al.[20]
- Or to a control group, in which the subjects had the same characteristics as the RME group but asked to postpone the RME.

Three-dimensional cone-beam computed tomography (CBCT) was captured at baseline (T0) with an iCat® machine (Imaging Sciences International, Hatfield, PA) following a standard protocol (120 kVp; 5 mA; field of view, 13 x 17 cm; voxel 0.4 mm; scan time, 20 seconds). Patients remained in maximum dental intercuspation during the acquisition of images, and the orientation of their head was decided according to the Frankfort and midsagittal planes.

All the appliances were manufactured by the same laboratory with 10 mm screws (Leone S.p.a, Italy- Ref. A2620-10) and stainless-steel wires soldered on the palatal surfaces of the maxillary first molars. The activation protocol required that screws be turned twice per day (0.25 mm per turn) for 1 week, then once per day for the second week and every other day for the third week until 20% overcorrection was achieved (T1). At T1, an occlusal radiography was done to ensure the opening of the mid-palatal suture, radiolucency, and increased width at the sutural site. The success of the procedure was assessed by the occurrence of an interincisal diastema. The Hyrax® expander was maintained for 6 months after the end of activation to stabilize the transverse dimension. Three-dimensional-CBCT was performed at 6 months (T2) for the control group and following expander removal in the RME group.

Individual data were reconstructed with 0.5 mm slice thickness. Viewbox 4 [Demetrios Halazonetis, developer of the software (dHAL software), Kifissia, Greece; www.dhal.com], was used to construct 3D surface models of the anatomic structures.

Radiographic Landmarks

T0 and T2 images of the two groups were captured, and the following 17 skeletal landmarks were used in the study with a three-dimensional (3D) identification procedure. Slices were scrolled in the frontal, axial and sagittal views until the most precise view of the structure and landmark were obtained using the gradient tool to define the best contour of bony structures and sutures (Fig. 1):

- *Nasion (Na)*: The most anterior aspect of the frontonasal suture from a sagittal view and centered mediolaterally from the axial and coronal views; (Figs 1A and B)
- *Anterior Nasal Spine (ANS)*: The most anterior point of the anterior nasal spine from the sagittal and axial views; (Figs 1C and D)
- *Sella (S)*: The center of the space in sella turcica from a sagittal view, centered mediolaterally on the base of sella turcica from the axial and coronal views; (Figs 1E and F)
- *Porion (Po right and left)*: The utmost aspect of the external auditory meatus; (Figs 1G and H)
- *Orbitale (Or right and left)*: The most inferior point of the orbital sphere; (Figs 1I and J)
- *External Acoustic Meatus (EAM right and left)*: The most lateral point of the posterior wall of the external acoustic meatus in the axial plane; (Figs 2A and B)
- *Center of the mandibular Condyle (CC right and left)*: The point at the middle of the condyle; (Figs 2C and D)
- *Laterosuperior Condyle (LSC right and left)*: Constructed point at the intersection of two lines tangent to the most lateral and superior border of the condyles; (Figs 2E and F)
- *Highest point of the Glenoid fossa (HG right and left)*: The upmost point of the glenoid fossa; (Fig. 2G)

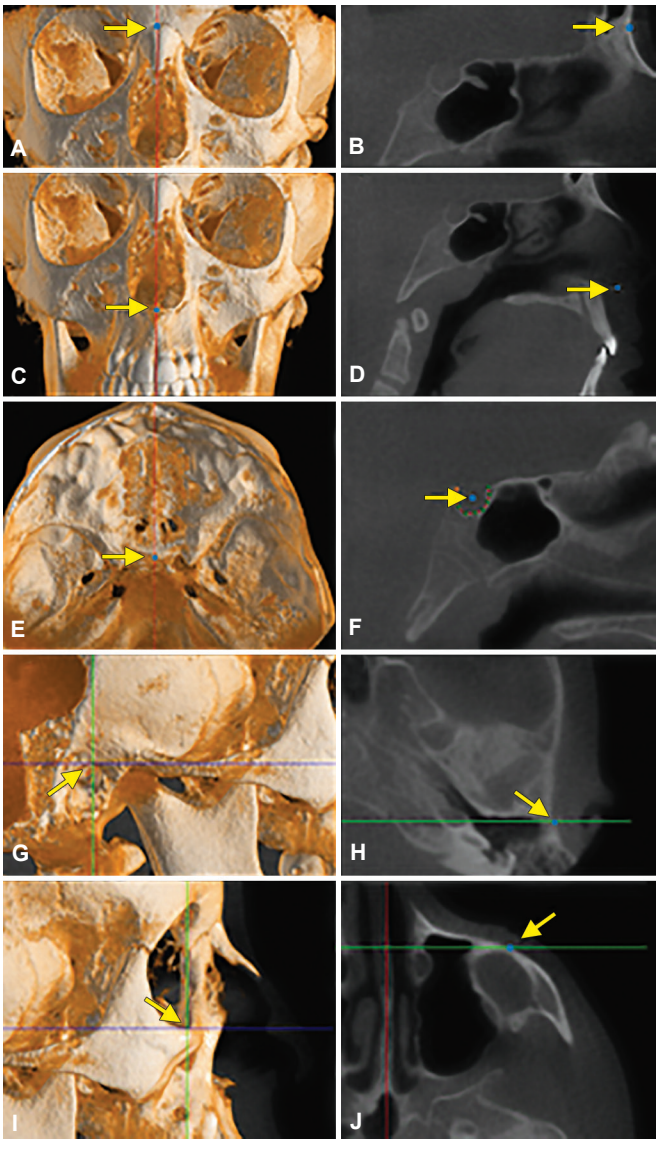

Figs 1A to J: Three-dimensional identification of landmarks. (A and B) Nasion (Na); (C and D) Anterior nasal spine (ANS); (E and F) Sella (S) identified using a curve following point by point the shape of the sella turcica on a sagittal view which center is localized automatically by the software; (G and H) Porion right and left (Po); (I and J) Orbitale right and left (Or)

- *Nasal Cavity (NC right and left)*: the most external point of the nasal cavity (Fig. 2H).

As described, all points were localized with respect to the coronal, axial, and sagittal planes; skeletal changes were determined by calculating distances between specific landmarks. To make possible comparisons of the measurements at different times indicating the displacement, the Frankfort and midsagittal planes were identified anatomically by localizing three landmarks for each: (Figs 3A to D)

- Frankfort plane joining Po right, Po left and the midpoint of the segment between Or right and Or left, this later calculated by the software;
- Midsagittal plane connecting Na, ANS, and S.

Thus, selection of landmarks, reference planes (Frankfort and Midsagittal) and center of curves chosen for sella turcica and mandibular condyles were included in a prespecified protocol for the dataset in the Viewbox 4 software (Fig. 4). Results were exported in CSV format to calculate the linear and angular changes for both groups at T0 and T2.

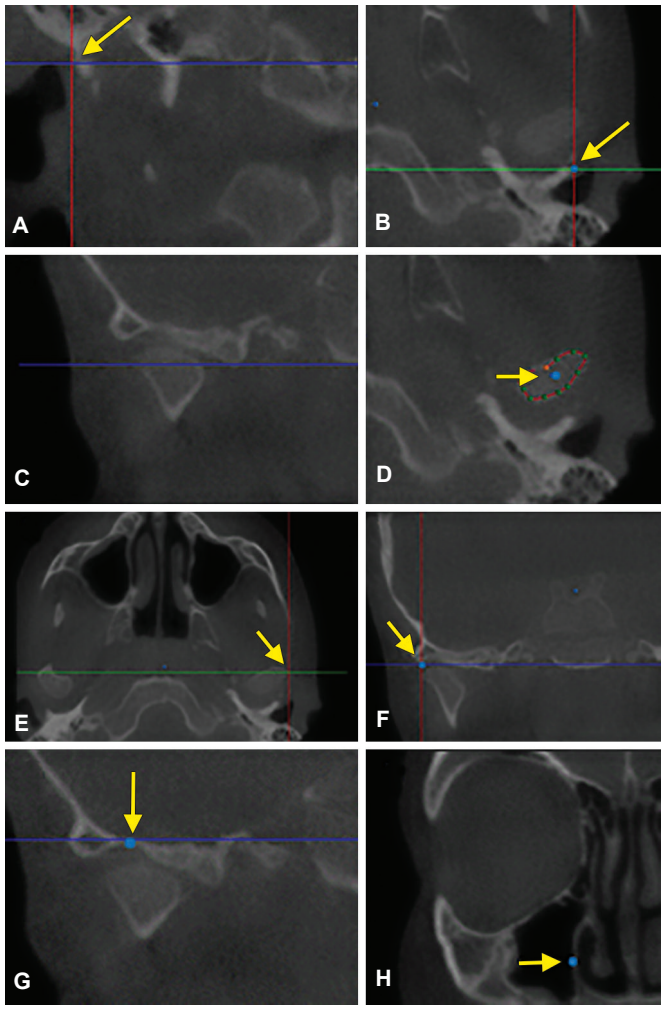

Figs 2A to H: (A and B) Three-dimensional identification of landmarks (continued). External acoustic meatus right and left (EAM): the most lateral point of the posterior wall of the external acoustic meatus in the axial plane; (C and D) CC right and left (Centre of the mandibular Condyle): first, the largest width of the condyle was identified on the frontal view. Next, based on an axial image, the chosen width was confirmed by scrolling in the axial view; then the contour of the condyle was chosen point by point to form a curve which centre was identified automatically by the software; (E and F) Laterosuperior condyle right and left (LSC): on the same axial view showing CC, identification of LSC was done at the widest point of the condyle then confirmed on a frontal view by intersecting two lines positioned tangentially to the most lateral and superior border of the condyles; (G) Highest point of the glenoid fossa right and left (HG): localized first on a 3D rendering sagittal view by setting the upmost point of the glenoid fossa, and then on a frontal view by scrolling until identifying the highest point of this structure; (H) Nasal cavity width right and left (NC): identified by scrolling on the coronal view until localizing the most external point of the nasal cavity

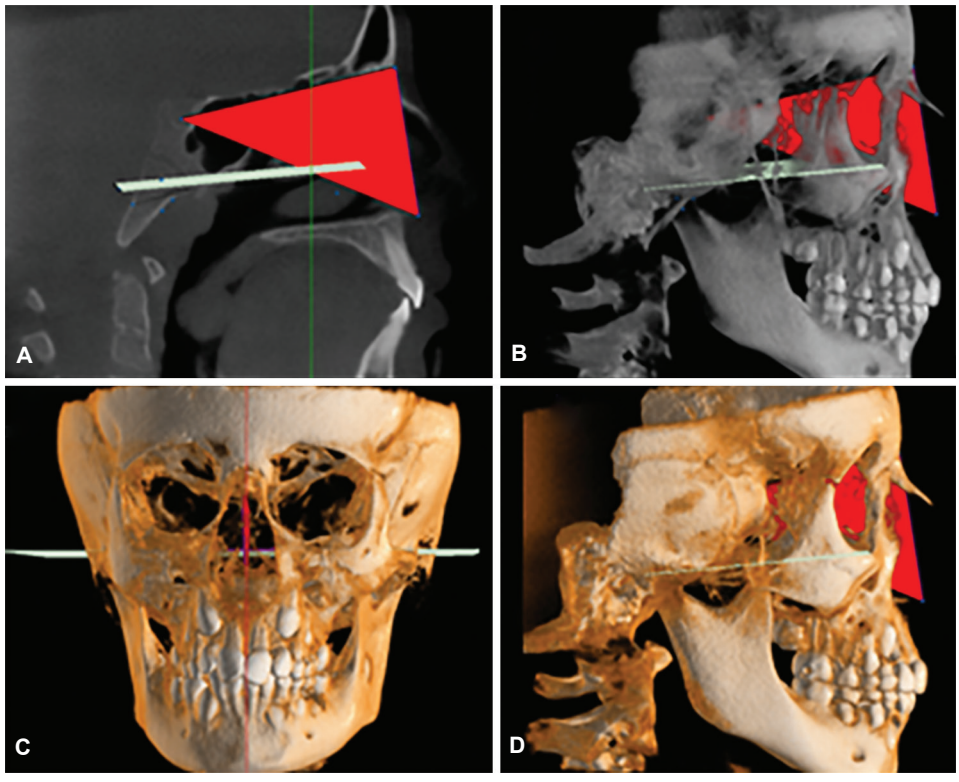

Figs 3 A to D: Reference planes: the midsagittal plane in red (Nasion, Na; Anterior nasal spine, ANS; and Center of sella turcica; S) and the Frankfort horizontal in light green (Porion right, Po right; Porion left, Po left; and the midpoint between orbitale right, or right and orbitale left, or left)

Clinical and Radiographic Parameters

The following measures were recorded on the right and left sides at T0 and T2 following Melgaço et al.,[10] except for the dimension 9:

- *Dimension 1*: The lateral position of the glenoid fossa, assessed on the coronal image: distance between the highest point of the glenoid fossa and the midsagittal plane (HG-Midsagittal plane distance).
- *Dimension 2*: The anteroposterior position of the condyles: evaluated on the horizontal distance between the external acoustic meatus and the center of the condyle, based on the sagittal image (EAM-CC horizontal distance).
- *Dimension 3*: Vertical position of the condyles: vertical distance between the EAM and the center of the condyle using the same sagittal image (EAM-CC vertical distance).
- *Dimension 4*: Laterolateral position of the condyles, based on the axial: distance between the center of the condyles and the midsagittal plane (CC-CC projected on the Midsagittal plane).
- *Dimension 5*: Vertical difference of the condyles, viewed on the coronal image: vertical difference of the center of the condyle landmarks when orthogonally projected on the midsagittal plane (CC projected right–CC projected left vertical distance on the Midsagittal plane).

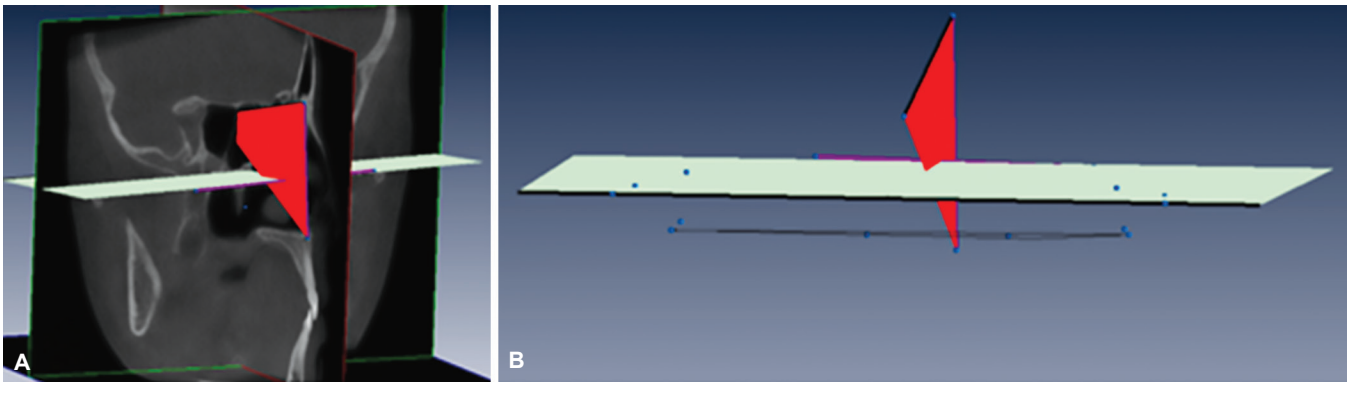

Figs 4A and B: Reference planes with all landmarks identified on the head volume rendering (A) and on the dataset image (B)

- *Dimension 6*: Anteroposterior difference of the condyles, assessed on the axial image: anteroposterior difference of the orthogonal projection of the center of the condyles landmarks on the midsagittal plane (CC projected right – CC projected left horizontal distance on the Midsagittal plane).
- *Dimension 7*: Axial condylar angle; considering the angle formed by the intersection of the line passing through the center of the condyle and the laterosuperior condyle landmarks with the midsagittal plane on the axial image. (3D axial condylar angle)
- *Dimension 8*: Coronal condylar angle; assessing the angle formed by the intersection of the line joining the center of the condyle and the laterosuperior condyle landmarks with the midsagittal plane on the coronal tomographic view. (3D coronal condylar angle)
- *Dimension 9*: Nasal width, assessed on the coronal image: distance between the widest point of the nasal fossa and the midsagittal plane. (NC-Midsagittal plane distance)

Intra- and inter-observer reliability were tested on five randomly selected patients from each group. Two operators (Principal Researcher, Mona S Ghoussoub and a student in master's degree in Orthodontics from LU) trained together and calibrated to identify 3D landmarks using CBCT scans not involved in this study. After calibration, they practiced independently marking landmarks on CBCT images also not part of the project at two different times and with an interval of 2 weeks. Results were compared to consider the reproducibility and reliability of the procedure which was confirmed to be able to test the intra and inter-examiner agreement. Subsequently, five CBCT images from the intervention group as well as five CBCT from the control one were analyzed and landmarks identified by both observers at T0 and T2. The results were compared to check, at 2 weeks interval, the intraobserver and interobserver conformity.

The primary outcome was the interglenoid fossa distance measured at T0 and T2. The secondary outcomes were:

- Condyle fossa relationship measured at T0 and T2
- 3D condylar angles measured at T0 and T2
- Nasal width measured at T0 and T2.

Sample Size

Using the Gpower® 3.1.9.2 software,[21] sample size calculation was based on the assumption of using an MANCOVA model, with an effect size f = 0.5 (based conservatively on the effect found at 3 weeks by Melgaço et al.),[10] an error probability = 5%, power of 90%, a two-group design with two repeated measures (T0, T2) and correlation among repeated measures of 0.7. While per protocol calculations yielded 38 patients, 27 patients were included during the study timeframe. Post-hoc observed power and effect size were recalculated.

Statistical Considerations

Lin's concordance correlation coefficient[22] was used to measure agreement. Since the measurements were naturally correlated with each other and were correlated to growth, and given the assessment at two different time points, a MANCOVA model was opted to control for type 1 family-wise error. For MANCOVA, the between-subject variable was the treatment group, and adjustment was made on age as a covariate. A time by group interaction term was included. Wilk's lambda was used for overall significance, and partial eta squared for effect sizes. Univariate F tests assessed the effect of each dependent variable (DV).

The first MANCOVA model assessed jointly the primary and secondary outcomes and included the following DVs:

- Lateral position of the glenoid fossa, average of dimension 1 (right, left)
- Anteroposterior position of the condyles, average of dimension 2 (right, left)
- Vertical position of the condyles, average of dimension 3 (right, left)
- Laterolateral position of the condyles, average of dimension 4 (right, left)
- Three-dimensional axial condylar angle, average of dimension 7 (right, left)
- Three-dimensional coronal condylar angle, average of dimension 8 (right, left)
- Nasal width, sum of dimension 9 (right, left)

The 2nd MANCOVA model explored asymmetry and included the following DVs:

- Vertical difference of the condyles (dimension 5)
- Anteroposterior difference of the condyles (dimension 6)
- Laterolateral difference of the condyles, (right, left) difference of dimension 4
- Asymmetry in 3D axial condylar angles, (right, left) difference of dimension 7
- Asymmetry in 3D coronal condylar angles, (right, left) difference of dimension 8
- Asymmetry in nasal width, (right, left) difference of dimension 9

The statistical analysis was performed using IBM SPSS.[23]

Table 1: Summary of the different CBCT measures used to assess the change effect (Changes measures) and the asymmetry effect (Asymmetry measures) between baseline (T0) and at 6-month follow-up (T2) SD: standard deviation; Min: minimum; Max: maximum

Dependent variables	*Control group*		*Expansion group*	
	N = 9		*N= 18*	
Changes measures	*Mean (SD)*	*Min - Max*	*Mean (SD)*	*Min - Max*
Lateral position of the glenoid fossa @ T0 (mm)	43.7 (2.2)	40.4–46.9	45.4 (2)	42.5–48.8
Lateral position of the glenoid fossa @ T2 (mm)	44.1 (1.8)	40.7–46	46.8 (1.8)	43.6–49.7
Anteroposterior position of the condyles @ T0 (mm)	7.7 (1.1)	5.7–9.5	8.4 (0.8)	6.7–9.9
Anteroposterior position of the condyles @ T2 (mm)	7.3 (1.6)	4.5–9.8	7.9 (0.9)	6.2–9.6
Vertical position of the condyles @ T0 (mm)	0.0 (0.2)	-0.4–0.2	0.1 (0.2)	-0.7–0.4
Vertical position of the condyles @ T2 (mm)	0.1 (0.1)	-0.1–0.2	0.1 (0.2)	-0.3–0.6
Laterolateral position of the condyles @ T0 (mm)	44 (2.1)	39.9–46.8	46 (1.7)	43–48.6
Laterolateral position of the condyles @ T2 (mm)	44.2 (1.9)	40.8–46.6	46.6 (1.9)	43–49.7
Nasal width @ T0 (mm)	28.2 (2.2)	25.4–32.4	28.9 (2.1)	25.3–34.5
Nasal width @ T2 (mm)	28.4 (2.9)	24.2–32.2	30.5 (2.1)	27.7–35.7
3D axial condylar angle @ T0 (degrees)	66.7 (4.1)	60.5–72.6	68.7 (4.9)	62.6–80.7
3D axial condylar angle @ T2 (degrees)	66.2 (3.3)	60.1–69.9	67.5 (3.6)	62.2–76.3
3D coronal condylar angle @ T0 (degrees)	71.6 (6.5)	62.4–79.2	66.9 (8.9)	50.3–80.4
3D coronal condylar angle @ T2 (degrees)	72.1 (7.0)	60.8–81.4	70.3 (7.3)	57.6–85.2
Asymmetry measures				
Vertical difference of the condyles @ T0 (mm)	0.0 (0.1)	-0.2–0.3	0.1 (0.2)	-0.2–0.5
Vertical difference of the condyles @ T2 (mm)	0.1 (0.3)	-0.2–0.6	0.3 (0.3)	-0.2–0.8
Anteroposterior difference of the condyles @ T0 (mm)	2.2 (2.7)	-2.5–6.9	0.2 (2.1)	-3.1–5.9
Anteroposterior difference of the condyles @ T2 (mm)	2.6 (2.5)	-1.3–6.2	-0.2 (2.5)	-4.7–4.1
Laterolateral difference of the condyles @ T0 (mm)	-1.6 (2.9)	-4.3–5	-2.1 (2.5)	-6.6–3.5
Laterolateral difference of the condyles @ T2 (mm)	-1.6 (2.4)	-5.9–1.6	-1.1 (3.5)	-9.6–7.2
Asymmetry in 3D Axial Condylar angle @ T0 (degrees)	1.9 (6.8)	-10.6–8.7	0.0 (5.4)	-13.6–7.4
Asymmetry in 3D Axial Condylar angle @ T2 (degrees)	0.9 (5.0)	-4.7–10.5	-1.6 (5.7)	-12.9–9.1
Asymmetry in 3D Coronal Condylar angle @ T0 (degrees)	-1.2 (10)	-21.4–14	-3.8 (7.1)	-25.8–9.6
Asymmetry in 3D Coronal Condylar angle @ T2 (degrees)	-5.8 (7.2)	-16.8–8.8	-4.0 (7.9)	-19.1–12.9
Asymmetry in Nasal width @ T0 (mm)	0.0 (1.5)	-1.9–2.3	-0.3 (0.9)	-2.3–1.6
Asymmetry in Nasal width @ T2 (mm)	0.6 (1.0)	-0.8–2.5	1.0 (2.6)	-1.5–8.7

RESULTS

The 27 patients included in the study had a mean age of 11.4 ± 1.5 years, and 16 (59.3%) among them were female. Intra- and inter-observer agreements were acceptable (all concordance correlation coefficients were >0.7). Table 1 depicts the different CBCT measures of change and asymmetry at T0 and T2.

For the change measures, MANCOVA analysis showed an overall group effect (p = 0.046, effect size 0.51) with a further group by time interaction (p = 0.012, effect size 0.59) as depicted in Table 2. Post-MANCOVA F-tests for interaction showed that the change in lateral position of the glenoid fossa, the primary outcome, was reached (p = 0.008, effect size 0.26). Of the secondary outcomes, change in the laterolateral position of the center of the condyle was significant (p=0.011, effect size = 0.24), and change in nasal cavity width tended towards significance (p = 0.065, effect size = 0.14). Variations of the different outcomes at T0 and T2 for both groups are shown in Graph 1.

For asymmetry assessment, MANCOVA analysis showed an overall group effect (p = 0.038, effect size 0.47) with no significant interaction (Table 3), driven essentially by asymmetry in the horizontal position of the condyles (p = 0.006, effect size 0.28), carried on from T0 until T2 with no effect of RME.

DISCUSSION

Most of the studies investigating the effects of RME on the facial and cranial structures are focusing on the direct

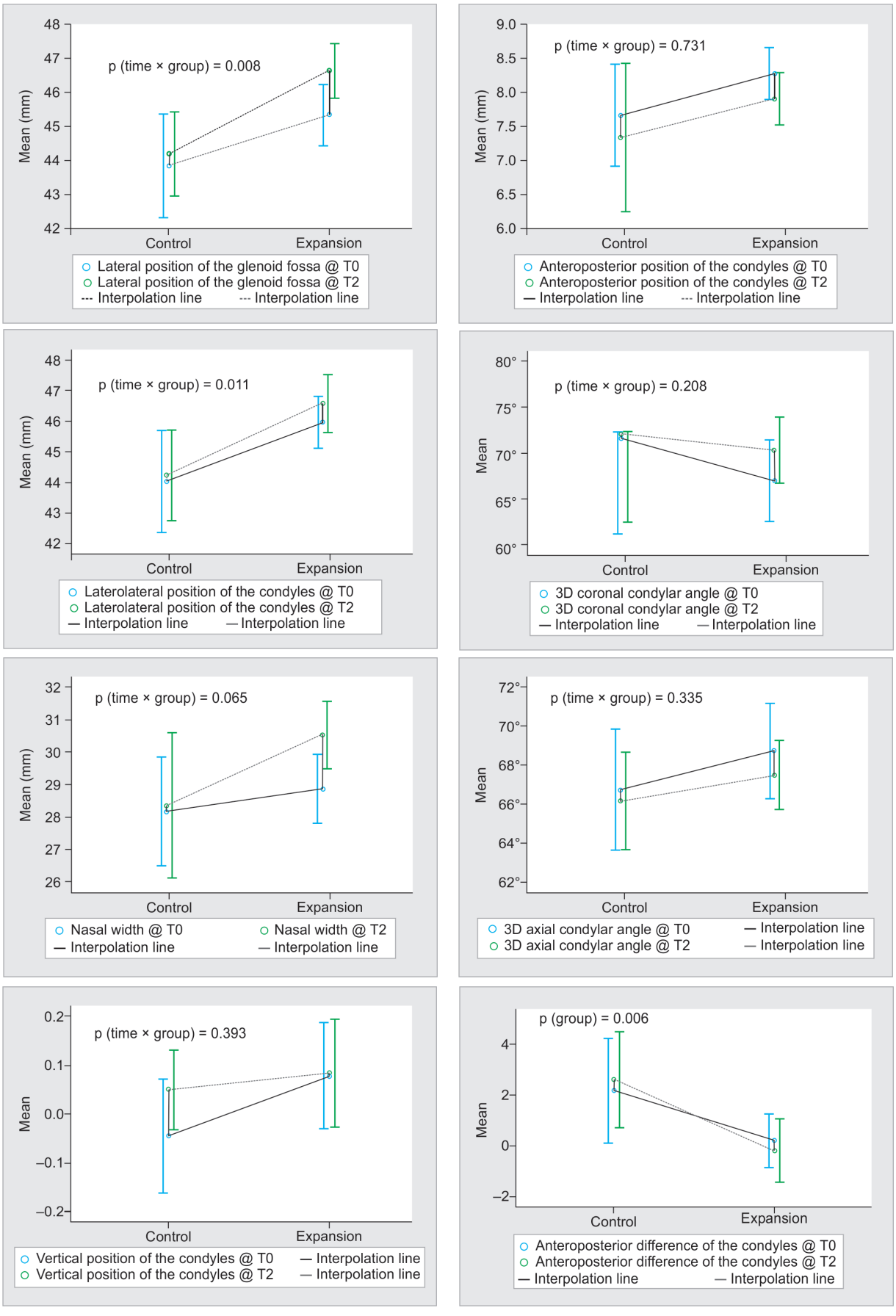

Graph 1: Variations of the defined CBCT distances between T0 (baseline) and T2 (6 months) in the 2 groups (study and control). The vertical bars represent 95% confidence intervals around the mean. Diagonal lines represent interpolation lines. A p-value is reported for each graph, corresponding to the one derived from the underlying MANCOVA model

Table 2: MANCOVA model 1 used to assess the change measures between baseline (T0) and at 6-month follow-up (T2)

(A): computed at alpha 5%

MANCOVA Model 1: Change Measures *Multivariate tests* *between subjects*	*Wilks' lambda*	*p-value*	*Partial eta²*	*Observed power[a]*
Intercept	0.033	0.000	0.967	100%
Age	0.559	0.107	0.441	61%
Group	0.493	0.046	0.507	75%
Within subjects				
Time	0.773	0.631	0.227	24%
Time x Age	0.836	0.818	0.164	17%
Time x Group	0.409	0.012	0.591	89%
Univariate Tests: Source: Time x Group				
lateral position of the glenoid fossa		0.008	0.258	0.792
Anteroposterior position of the condyles		0.731	0.005	0.063
Vertical position of the condyles		0.393	0.031	0.133
Laterolateral position of the condyles		0.011	0.242	0.756
3D axial condylar angle		0.335	0.039	0.157
3D coronal condylar angle		0.208	0.065	0.237
Nasal width		0.065	0.135	0.459

impact of this procedure on the maxillary arch site of the expansion device, and on the surrounding anatomical structures. Thus, the opening of the palatal and circumaxillary sutures were extensively inspected using 3D imaging and sophisticated software to assess consequent changes.[13,14,23]

Few studies were done on the effect of RME on the mandibular condyle which could be altered after RME attempting to adjust to the interglenoid fossa increase, considering that the potential of remodeling is high at this age. Studies by Kecik et al.[14] found that the condyles that were initially malpositioned in the glenoid fossa have become symmetrical after expansion treatment using documents such as lateral, posteroanterior, submentovertex cephalograms, transcranial temporomandibular joint radiographs, joint vibration analysis, electromyographic recordings, and magnetic resonance images for every patient before and after maxillary expansion and at one point for the controls but not three-dimensional CBCT. In a similar pattern, Arat et al.[15] used MRI in patients undergoing maxillary expansion treatment and concluded that this treatment has an impact on condylar

Table 3: MANCOVA model 2 used to assess the asymmetry measures between baseline (T0) and at 6-month follow-up (T2)

(A): computed at alpha 5%

MANCOVA Model 2: Asymmetry Measures *Multivariate tests* *between subjects*	*Wilks' lambda*	*p-value*	*Partial eta²*	*Observed power[a]*
Intercept	0.767	0.478	0.233	29%
Age	0.747	0.412	0.253	32%
Group	0.528	0.038	0.472	76%
Within subjects				
Time	0.803	0.599	0.197	23%
Time x Age	0.765	0.470	0.235	29%
Time x Group	0.884	0.860	0.116	14%
Tests of between-subject effects	Source: Group			
Vertical difference of the condyles		0.201	0.067	24%
Anteroposterior difference of the condyles		0.006	0.277	83%
Laterolateral difference of the condyles		0.680	0.007	7%
Asymmetry in 3D axial condylar angle		0.077	0.125	43%
Asymmetry in 3D coronal condylar angle		0.783	0.003	6%
Asymmetry in nasal width		0.765	0.004	6%

response without giving any precision whether the effect was beneficial or not.

Recently, two publications have used 3D-CBCT and reported an association between RME and temporomandibular joints (TMJs) changes concerning width increase of the interglenoid fossa distance and spatial mandibular adaptation to this movement.[10,12] Patients' mean age in the study of Melgaço et al. was 12 years 10 months for girls and 13 years for boys,[10] and for McLeod et al. 14 years ±1 for the study group and 13 years ±1 for the control group.[12] In the current study, the mean age was of 11.4±1.5 years inferior to the two previous reports, potentially leading to a midpalatal suture that would respond more efficiently at an earlier age, with an impact on the TMJ that could be greater. In addition, subjects included in the current study exhibited bilateral crossbite, revealing a true transverse deficiency of the maxilla and a more functional need for expansion. This factor was not involved in the inclusion criteria of the two previous reports.

In the assessment of the primary outcome, results demonstrated significant increase of the interglenoid fossa distance in youngsters. Consequently, the primary objective of the study showed that the transversal change after RME is not only affecting the facial bones adjacent to the midpalatal sutures [24,25] but has also an impact on more distant areas such as the temporal bone.[14]

Among secondary outcomes also, the intercondylar distance demonstrated a significant transverse increase, while the 3D coronal and axial angles were comparable, implying a laterolateral translation of the condyles in adaptation to the temporal interglenoid fossa distance augmentation. Anteroposterior and vertical positions of the condyles were comparable in both groups. In the study of Melgaço et al.,[10] CBCT images were collected before activation of the expander and 3 weeks later, after screw stabilization, which could be considered short-term to make possible evaluation of the dimensional skeletal adaptation at the temporomandibular joints. In the current study, the period between T0 and T2 was at least six months allowing to consider not only immediate condylar alteration but also the bony remodeling in the condyle-fossa relationship.

While Melgaço et al.[10] used Dolphin imaging software (version 11.0; Dolphin Imaging and Management Solutions, Chatsworth, Calif) to determine and reproduce head positioning and landmarks during the sequential times of the study, we opted for a new customized radiological technique designed to select landmarks by scrolling in the three-dimensions to determine precise anatomical reference planes and calculate accurately changes at T0 and T2. Mcleod et al.[12] study aimed to investigate the presence of condylar spatial changes in patients having RME treatments compared to a control group. CBCTs were analyzed using AVIZO, general-purpose commercial software application for scientific and industrial data visualization and analysis software and landmarks were positioned on the upper first molars and premolars, cranial base, condyles, and glenoid fossa. Descriptive statistics revealed that changes in the mandibular condylar position with respect to the glenoid fossa were insignificant in both groups. The largest difference was attained when measuring the distance between the left and right condyle heads. When comparing changes between both groups, no statistically significant difference was found between changes in the condyles.

Similarly, during the acquisition of scanned images at T0 and T2, the patient remained in centric occlusion. In this position, the condylar changes seem more related to the occlusal alteration. We investigated the effect of RME on the condyles at least six months after screw stabilization waiting for a possible adaptation of the mandibular condyle to the expansion at the level of the glenoid fossa and also of the reorientation of the mandibular teeth to adapt to the maxillary arch enlargement. The results demonstrated an overall significant group effect in the asymmetry assessment essentially in the horizontal position of the condyles even though metric measurements showed no abnormal pattern. These findings are in concordance with those of Hesse et al.[13] where the condyles moved in an asymmetric fashion when applying RME treatment.

In summary, RME treatments using a tooth-anchored appliance (hyrax) do not give rise to significant condylar positional changes with respect to the glenoid fossa when compared to a non-treated control group after appliance removal (6 months) thus not representing a limitation for employing this treatment.

Limitations of the Study

Random allocation was not possible, the subjects' preference to be allocated to a particular group was respected. Subjects in the control group were selected from the same population as the treatment group, which lessens selection bias. Furthermore, adjustment on covariates in the statistical analysis was performed to help controlling bias.

Blinding was not feasible with the presence of the device. However, choosing quantitative measures, assessed by independent evaluators helped in limiting this bias. The pre-specified sample size was not reached for the recruitment dropped in the accessible population. However, observed effect sizes and power values matched the pre-specified ones.

CONCLUSION

The current study shows that RME is effective during growth, widening the interglenoid fossa distance and the lateral positions of the condyles and enlarging the nasal cavity, without significant asymmetry. Further studies are needed to help correlate these findings with enhanced nasal breathing, increased hearing, less obstructive sleep apnoea, less frequent temporomandibular disorders and dental malocclusion.

ACKNOWLEDGMENTS

The study was funded jointly by the Lebanese CNRS (Centre National de Recherche Scientifique) and the Lebanese University under the registration number: 652-14/04/2016. These institutions had no role in the design of the study, neither collection, analysis, nor interpretation of data or in writing the manuscript.

REFERENCES

1. Haas AJ. Palatal expansion: just the beginning of dentofacial orthopedics. Am J Orthod. 1970;57(3):219-255.
2. Haas AJ. Rapid expansion of the maxillary dental arch and nasal cavity by opening the midpalatal suture. Angle Orthod. 1961;31:73-90.
3. Bishara SE, Staley RN. Maxillary expansion: clinical implications. Am J Orthod Dentofac Orthop Off Publ Am Assoc Orthod Its Const Soc Am Board Orthod. 1987;91(1):3-14.
4. Bazargani F, Jönson-Ring I, Nevéus T. Rapid maxillary expansion in therapy-resistant enuretic children: An orthodontic perspective. Angle Orthod. 2016;86(3):481-486.
5. Kumar PS. Diversity of Oral Biofilms in Periodontal Health and Disease. Pathogenesis of Periodontal Diseases [Internet]. Springer International Publishing; 2017 Jul 12;9–20.
6. Taşpinar F, Uçüncü H, Bishara SE. Rapid maxillary expansion and conductive hearing loss. Angle Orthod. 2003;73(6):669-673.
7. Bell RA, LeCompte EJ. The effects of maxillary expansion using a quad-helix appliance during the deciduous and mixed dentitions. Am J Orthod. 1981;79(2):152-161.
8. Timms DJ. A study of basal movement with rapid maxillary expansion. Am J Orthod. 1980;77(5):500-507.
9. Leonardi R, Sicurezza E, Cutrera A, Barbato E. Early post-treatment changes of circumaxillary sutures in young patients treated with rapid maxillary expansion. Angle Orthod. 2011;81(1):36-41.
10. Melgaço CA, Columbano Neto J, Jurach EM, Nojima M da CG, Nojima LI. Immediate changes in condylar position after rapid maxillary expansion. Am J Orthod Dentofac Orthop Off Publ Am Assoc Orthod Its Const Soc Am Board Orthod. 2014;145(6):771-779.
11. Oberheim MC, Mao JJ. Bone strain patterns of the zygomatic complex in response to simulated orthopedic forces. J Dent Res. 2002;81(9):608-612.
12. McLeod L, Hernández IA, Heo G, Lagravère MO. Condylar positional changes in rapid maxillary expansion assessed with cone-beam computer tomography. Int Orthod. 2016;14(3):342-356.
13. Hesse KL, Artun J, Joondeph DR, Kennedy DB. Changes in condylar postition and occlusion associated with maxillary expansion for correction of functional unilateral posterior crossbite. Am J Orthod Dentofac Orthop 1997;111(4):410-418.
14. Kecik D, Kocadereli I, Saatci I. Evaluation of the treatment changes of functional posterior crossbite in the mixed dentition. Am J Orthod Dentofac Orthop 2007;131(2):202-215.
15. Arat FE, Arat ZM, Tompson B, Tanju S, Erden I. Muscular and condylar response to rapid maxillary expansion. Part 2: magnetic resonance imaging study of the temporomandibular joint. Am J Orthod Dentofac Orthop 2008;133(6):823-829.
16. Işeri H, Tekkaya AE, Oztan O, Bilgiç S. Biomechanical effects of rapid maxillary expansion on the craniofacial skeleton, studied by the finite element method. Eur J Orthod. 1998;20(4):347-356.
17. Jafari A, Shetty KS, Kumar M. Study of stress distribution and displacement of various craniofacial structures following application of transverse orthopedic forces--a three-dimensional FEM study. Angle Orthod. 2003;73(1):12-20.
18. Priyadarshini J, Mahesh CM, Chandrashekar BS, Sundara A, Arun AV, Reddy VP. Stress and displacement patterns in the craniofacial skeleton with rapid maxillary expansion-a finite element method study. Prog Orthod. 2017;18(1):17.
19. Sayegh-Ghoussoub M. Effect of rapid xaxillary expansion on glenoid fossa and condylar position in growing patients. http://isrctn.com/ [Internet]. Springer Nature; 2017 Nov 7.
20. Primožič J, Richmond S, Kau CH, Zhurov A, Ovsenik M. Three-dimensional evaluation of early crossbite correction: a longitudinal study. Eur J Orthod. 2013;35(1):7-13.
21. Faul F, Erdfelder E, Lang A-G, Buchner A. G*Power 3: a flexible statistical power analysis program for the social, behavioral, and biomedical sciences. Behav Res Methods. 2007;39(2):175-191.
22. Lin LI. A concordance correlation coefficient to evaluate reproducibility. Biometrics. 1989;45(1):255-268.
23. Lagravère MO, Low C, Flores-Mir C, et al. Intraexaminer and interexaminer reliabilities of landmark identification on digitized lateral cephalograms and formatted 3-dimensional cone-beam computerized tomography images. Am J Orthod Dentofac Orthop 2010;137(5):598-604.
24. Isaacson R, Ingram A. Forces produced by rapid maxillary expansion. Part II. Forces present during treatment. Angle Orthod. 1964;34:261-270.
25. Isaacson R, Wood J, Ingram A. Forces produced by rapid maxillary expansion. Part I. Design of the force measuring system. Angle Orthod. 1964;34:256–260.